




# Solid-State Phase Equilibria at 320°C of the Mg-Gd-Zn System in the Region of Less Than 50 at.% Gd

HONGHUI XU,<sup>1</sup> TAO ZHOU,<sup>1</sup> PEISHENG WANG <sup>1,2,3</sup>  
WEI YANG,<sup>1</sup> and KUN LIU<sup>1</sup>

1.—State Key Laboratory of Powder Metallurgy, Central South University, Changsha 410083, People's Republic of China. 2.—Hunan Key Laboratory of Advanced Fibers and Composites, Central South University, 410083 Changsha, People's Republic of China. 3.—e-mail: peisheng.wang@outlook.com

Phase equilibria of the Mg-Gd-Zn system at 320°C are important because it has been reported that the aging treatment is carried out at that temperature. The phase equilibria at 320°C for the Mg-Zn side ( $x(\text{Gd}) < 50$  at.%) were investigated with equilibrated alloys using electron probe microanalysis and X-ray diffraction. The partial isothermal section ( $x(\text{Gd}) < 50$  at.%) was constructed. Eight ternary phases,  $\tau_1$  to  $\tau_8$ , were observed at 320°C. The W phase ( $\text{Gd}_2\text{Mg}_3\text{Zn}_3$ ) which was found at high temperatures in the literature was not observed at 320°C. The analysis of the present data also indicates that the icosahedral quasicrystalline (I phase) in the Mg-Gd-Zn system is not stable. One important solid transition was found in the present work: the three-phase equilibria  $(\text{Mg}) + \text{GdMg}_3 + \text{GdMg}_5$  and  $(\text{Mg}) + \text{GdMg}_3 + \tau_1$  at 500°C transform to  $(\text{Mg}) + \text{GdMg}_5 + \tau_1$  and  $\text{GdMg}_5 + \tau_1 + \text{GdMg}_3$  at 320°C, due to the invariant reaction of  $(\text{Mg}) + \text{GdMg}_3 \rightarrow \text{GdMg}_5 + \tau_1$ .

## INTRODUCTION

Mg-Gd-Zn magnesium alloys have received much attention due to their high strength at high temperatures and good corrosion resistance.<sup>1,2</sup> Many studies have been carried out on the long period stacking ordered (LPSO) phase,<sup>3–5</sup> icosahedral quasicrystalline phase (I-phase),<sup>6–9</sup> and aging precipitation<sup>10,11</sup> in Mg-Gd-Zn magnesium alloys. It is generally recognized that the applications of phase diagrams can significantly accelerate the development of high-performance magnesium alloys, through the predictions of the phase transitions, microstructure evolutions, and heat treatment processes (e.g., homogenization and aging, etc.).

The phase equilibria of the Mg-Gd-Zn system above 400°C have been studied by several groups of researchers.<sup>12–17</sup> For example, the phase equilibria at 500°C in the region of  $x(\text{Gd}) < 50$  at.% were investigated in our previous work.<sup>17</sup> However, the solid phase equilibria at lower temperatures (below

400°C) have not been studied. It has been reported that the aging treatment for the Mg-Zn-RE (rare earth) alloys in the temperature range of 200–350°C can significantly improve strength. Thus, understanding the phase equilibria of the Mg-Gd-Zn system in that temperature range is important. Thus, this study aims to determine the solid-state phase equilibria at 320°C in the region of  $x(\text{Gd}) < 50$  at.%.

## EXPERIMENTAL DETAILS

Thirty-eight Mg-Gd-Zn alloys, listed in Table I, were synthesized. High-purity magnesium (99.99 wt.%), zinc (99.999 wt.%), and gadolinium (99.9 wt.%) were used as the raw materials. Before weighing, the oxide layers on the surfaces of the magnesium, zinc, and gadolinium blocks were mechanically removed. The accurately weighed and cleaned materials of the Zn, Mg, and Gd blocks were sealed into Ta crucibles with argon gas (99.999 wt.%) which were then separately sealed into quartz tubes with argon gas (99.999 wt.%). The preparation of the alloys was as described in our previous study.<sup>18</sup> Alloys that are marked with superscript

**Table I. Summary of the experimental information and results on the phase equilibria in the alloys annealed at 320°C**

No.	Nominal composition <sup>a</sup> Mg Gd Zn (Annealing time) <sup>b</sup>	Measured composition (at.%, balance: Mg)		
		Phase 1 Gd Zn	Phase 2 Gd Zn	Phase 3 Gd Zn
1 <sup>c</sup>	89.7 7.5 2.8 (300 days)	(Mg) 0.7 0.1 $\tau_1$ (14H) 7.4 5.4	GdMg <sub>5</sub> 13.2 0.8 GdMg <sub>5</sub> 15.5 1.6	$\tau_1$ (14H) 6.1 4.4 GdMg <sub>3</sub> 20.7 6.9
2 <sup>c</sup>	82.0 13.5 4.5 (300 days)	$\tau_1$ (14H) 7.8 5.5 $\tau_1$ (14H) 6.5 4.7	GdMg <sub>5</sub> 15.6 1.6 (Mg) 0.5 0.2	GdMg <sub>3</sub> 20.7 7.0
3	75.5 21.0 3.5 (300 days)	GdMg <sub>3</sub> 21.8 4.6	GdMg <sub>5</sub> 16.6 1.0	
4 <sup>c</sup>	73.7 15.3 11.0 (300 days)	$\tau_1$ (14H) 7.2 5.5	GdMg <sub>3</sub> 21.7 15.6	
5 <sup>c</sup>	71.9 15.3 12.8 (300 days)	$\tau_1$ (14H) 7.1 5.3	GdMg <sub>3</sub> 22.7 21.2	
6 <sup>c</sup>	59.0 20.5 20.5 (300 days)	$\tau_1$ (14H) 7.0 5.2	GdMg <sub>3</sub> 23.2 25.4	
7 <sup>c</sup>	45.1 22.7 32.2 (300 days)	$\tau_1$ (14H) 6.7 5.1	GdMg <sub>3</sub> 23.7 34.1	
8	88.8 5.6 5.6 (100 days)	(Mg) 0.2 0.3	$\tau_1$ (14H) 5.5 4.3	GdMg <sub>3</sub> 23.6 38.2
9	45.0 14.0 41.0 (300 days)	(Mg) 0.1 1.3	GdMg <sub>3</sub> 24.4 49.1	$\tau_5$ (F-phase) 14.3 61.1
10	41.5 8.5 50.0 (300 days)	(Mg) 0.1 2.5	$\tau_2$ (Z-phase) 7.8 60.8	$\tau_5$ (F-phase) 13.6 62.1
11	70.6 1.4 28.0 (100 days)	(Mg) 0.0 3.1	$\tau_2$ (Z-phase) 6.8 63.0	MgZn 0.1 50.1
12	40.0 2.0 58.0 (300 days)	$\tau_2$ (Z-phase) 6.4 64.2	MgZn 0.1 51.6	Mg <sub>2</sub> Zn <sub>3</sub> 0.1 58.9
13	34.7 1.2 64.1 (100 days)	Mg <sub>2</sub> Zn <sub>3</sub> 0.5 59.8	MgZn <sub>2</sub> 0.7 65.7	$\tau_2$ (Z-phase) 6.4 65.3
14 <sup>c</sup>	13.3 7.5 79.2 (300 days)	MgZn <sub>2</sub> 0.5 66.4	$\tau_2$ (Z-phase) 6.5 66.8	Gd <sub>2</sub> Zn <sub>17</sub> 10.4 88.3
15	17.0 2.0 81.0 (300 days)	MgZn <sub>2</sub> 0.1 67.5	Mg <sub>2</sub> Zn <sub>11</sub> 0.1 84.7	GdZn <sub>12</sub> 7.6 92.4
16	8.7 1.3 90.0 (100 days)	Mg <sub>2</sub> Zn <sub>11</sub> 0.1 84.9	GdZn <sub>12</sub> 7.5 92.5	(Zn) 0.1 99.8
17	24.0 12.5 63.5 (300 days)	$\tau_2$ (Z-phase) 8.5 63.5	$\tau_4$ 11.4 64.4	$\tau_5$ (F-phase) 13.7 63.6
18 <sup>c</sup>	23.5 11.5 65.0 (300 days)	$\tau_2$ (Z-phase) 8.3 64.5	$\tau_3$ 10.4 65.0	$\tau_4$ 11.3 64.9
19	21.5 11.5 67.0 (300 days)	$\tau_3$ 10.6 65.2	$\tau_4$ 11.4 65.1	$\tau_5$ (F-phase) 13.9 65.3
		$\tau_3$ 10.6 65.4	$\tau_5$ (F-phase) 14.0 65.6	$\tau_6$ 13.8 70.4
		$\tau_2$ 8.2 64.9	$\tau_3$ 10.5 65.5	$\tau_6$ 13.6 70.7
		$\tau_3$ 10.7 64.8	$\tau_4$ 11.5 64.8	$\tau_5$ 14.2 64.9
20	19.0 11.5 69.5	$\tau_2$ (Z-phase) 7.8 65.9	$\tau_6$ 13.4 72.7	
21 <sup>c</sup>	13.0 12.0 75.0 (300 days)	$\tau_2$ (Z-phase) 7.4 67.4	$\tau_6$ 13.3 74.0	Gd <sub>2</sub> Zn <sub>17</sub> 10.5 86.3
22 <sup>c</sup>	1.2 12.0 86.8 (100 days)	Gd <sub>2</sub> Zn <sub>17</sub> 10.6 88.1	Gd <sub>13</sub> Zn <sub>58</sub> 17.1 82.5	Gd <sub>3</sub> Zn <sub>22</sub> 12.5 86.8

Table I. continued

No.	Nominal composition <sup>a</sup>		Measured composition (at.%, balance: Mg)		
	Mg Gd Zn (Annealing time) <sup>b</sup>		Phase 1	Phase 2	Phase 3
			Gd Zn	Gd Zn	Gd Zn
23	3.5 13.5 83.0 (300 days)	$\tau_8$ 16.1 78.6	Gd <sub>13</sub> Zn <sub>58</sub> 17.3 80.3	Gd <sub>2</sub> Zn <sub>17</sub> 10.6 86.9	
24	6.5 16.0 77.5 (300 days)	$\tau_6$ 14.2 74.3	$\tau_8$ 16.1 77.4	Gd <sub>13</sub> Zn <sub>58</sub> 17.4 77.8	
25	9.7 16.3 74.0 (300 days)	$\tau_6$ 14.4 73.6	$\tau_7$ 16.3 73.3	Gd <sub>13</sub> Zn <sub>58</sub> 17.5 76.1	
26)	16.0 14.5 69.5 (300 days)	$\tau_5$ (F-phase) 14.9 66.7	$\tau_6$ 14.4 71.4	$\tau_7$ 16.4 68.6	
27	21.4 15.2 63.4 (300 days)	GdMg <sub>3</sub> 24.8 50.5	$\tau_5$ (F-phase) 14.9 64.1		
28 <sup>c</sup>	17.5 17.0 65.5 (300 days)	$\tau_5$ (F-phase) 15.1 65.7	$\tau_7$ 16.5 66.3	GdMg <sub>3</sub> 24.7 51.4	
29	9.0 21.0 70.0 (300 days)	$\tau_7$ 16.7 69.5	GdMg <sub>3</sub> 24.6 51.7	Gd <sub>13</sub> Zn <sub>58</sub> 17.8 75.3	
		$\tau_5$ (F-phase) 15.1 66.1	$\tau_7$ 16.5 66.9	GdMg <sub>3</sub> 24.8 51.3	
		$\tau_7^d$ 16.5 69.2	GdMg <sub>3</sub> <sup>d</sup> 24.8 51.7	Gd <sub>3</sub> Zn <sub>11</sub> <sup>d</sup> 21.6 74.8	
30	6.5 20.5 73.0	GdMg <sub>3</sub> 25.0 51.6	Gd <sub>13</sub> Zn <sub>58</sub> 18.2 75.1	Gd <sub>3</sub> Zn <sub>11</sub> 21.5 75.2	
		$\tau_7^d$ 16.4 69.6	Gd <sub>13</sub> Zn <sub>58</sub> <sup>d</sup> 18.1 75.4	Gd <sub>3</sub> Zn <sub>11</sub> <sup>d</sup> 21.5 75.3	
		GdMg <sub>3</sub> 25.1 51.7	Gd <sub>3</sub> Zn <sub>11</sub> 21.4 76.6	GdZn <sub>3</sub> 24.9 75.1	
31 <sup>c</sup>	7.5 23.5 69.0 (300 days)	GdMg <sub>3</sub> 25.2 51.4	GdZn <sub>2</sub> 33.0 67.0	GdZn <sub>3</sub> 25.0 75.0	
32	4.0 29.0 67.0 (300 days)	GdMg <sub>3</sub> 25.3 47.1	GdZn <sub>2</sub> 33.4 66.6	Gd(MgZn) 46.3 49.3	
33	11.0 37.0 52.0 (300 days)	GdMg <sub>3</sub> 25.1 40.3	Gd(MgZn) 46.8 44.6		
34	27.5 30.0 42.5 (300 days)	GdMg <sub>3</sub> 25.2 32.8	Gd(MgZn) 47.1 39.1		
35 <sup>c</sup>	40.0 27.3 32.7 (300 days)	GdMg <sub>3</sub> 25.1 20.2	Gd(MgZn) 47.2 26.3		
36	52.0 27.5 20.5 (300 days)	GdMg <sub>3</sub> 25.3 11.8	Gd(MgZn) 47.5 15.2		
37	41.0 44.0 15.0 (300 days)	GdMg <sub>3</sub> 25.1 8.9	GdMg <sub>2</sub> 32.3 0.8	Gd(MgZn) 47.0 11.5	
38	60.5 32.5 7.0 (300 days)				

<sup>a</sup>Nominal composition of the alloys (in at.%). <sup>b</sup>Annealing time at 320°C. <sup>c</sup>The alloys from the previous work at 500°C.<sup>17</sup> <sup>d</sup>The data are not in agreement with the presently established isothermal section.

“c” in Table I were taken from the previous work.<sup>17</sup> These alloys were cooled from 500°C to 320°C in 20 h, and then were re-sealed individually in the Ta crucibles, which were then put into in the quartz tubes. All the alloys in Table I were annealed at 320°C for 100 ~ 300 days, and then quenched in cold water. To increase the cooling rate of the samples, the quartz tubes were quickly broken after being dropped into the cold water.

The metallographic samples of the alloys were prepared under ethanol, and then characterized by an electron probe microanalyzer (JXA-8530F; JEOL, Japan) at 15 kV and  $2 \times 10^{-8}$  A, with pure

Mg (99.99 wt.%), Zn (99.999 wt.%), and GdF<sub>3</sub> as standard materials for calibration. The equilibrium compositions of the phases in Table I were obtained by the method described in Ref. 19. X-ray powder diffraction (XRD) was performed for the alloys.

## EXPERIMENTAL RESULTS AND DISCUSSION

Table I presents the nominal alloy compositions, the identified phases, and the determined phase compositions.

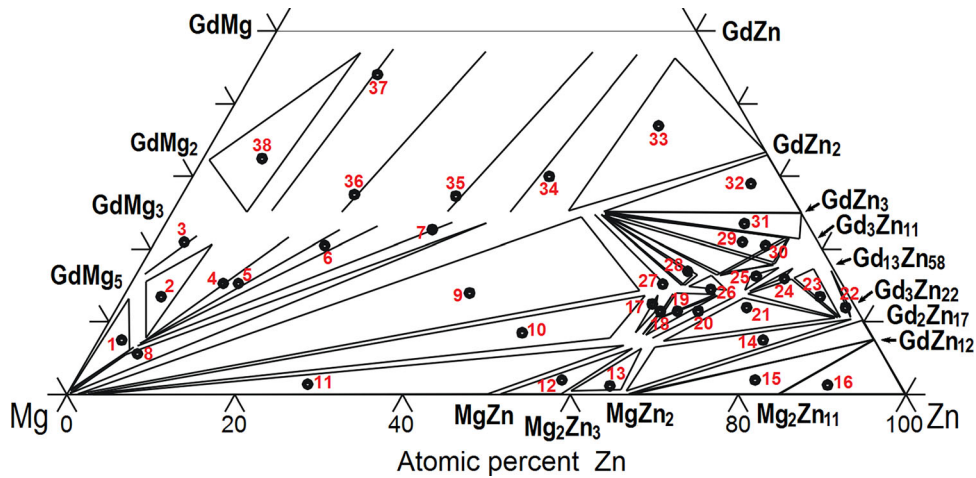


Fig. 1. Experimentally determined tie-lines and tie-triangles as well as the alloy positions with numbers.

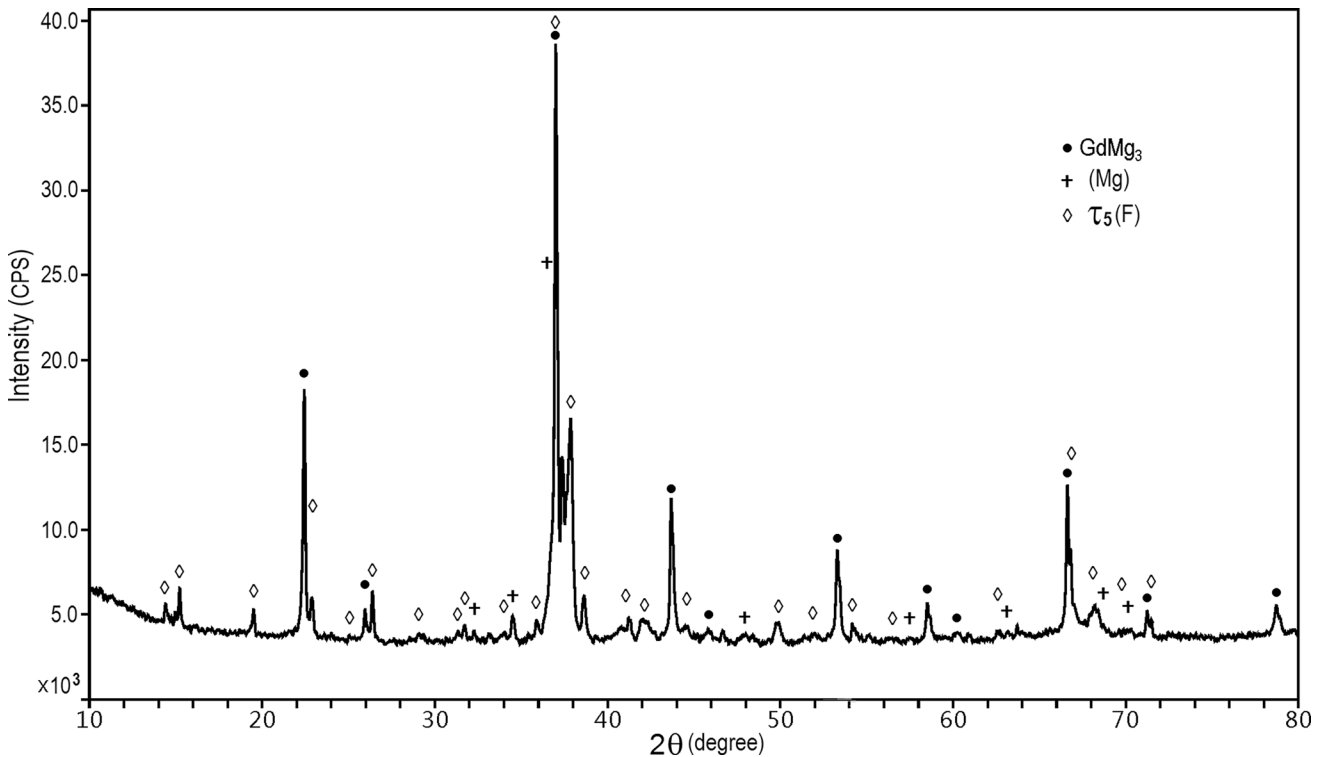


Fig. 2. XRD patterns of alloy #9.

Figure 1 shows the phase compositions as listed in Table I. The XRD patterns and backscattered electron (BSE) images of some representative alloys are presented in Figs. 2 and 3, respectively. The partial isothermal section ( $x(\text{Gd}) < 50$  at.%) at  $320^\circ\text{C}$  is constructed in Fig. 4. The  $\text{GdMg}$  and  $\text{GdZn}$  phases with the same crystal structure form a continuous solid solution, denoted as  $\text{Gd}(\text{Mg}, \text{Zn})$ . The solid and dashed lines in Fig. 4 represent the measured tie-triangles in the present work and the extrapolated ones, respectively.

### Ternary Compounds

Eight ternary compounds, labeled as  $\tau_1$  to  $\tau_8$ , were observed. Table II summarizes the compositions and crystallographic data of the ternary compounds. The W and I phases, which were found in the literature, were not found in the present work.

The  $\tau_1$  phase, labeled as the X-phase in some references,<sup>12–14</sup> has a LPSO. It has been reported that the precipitation of the LPSO  $\tau_1$  phase can significantly increase the strength of Mg-Zn-RE alloys. The homogeneity range of the  $\tau_1$  phase has

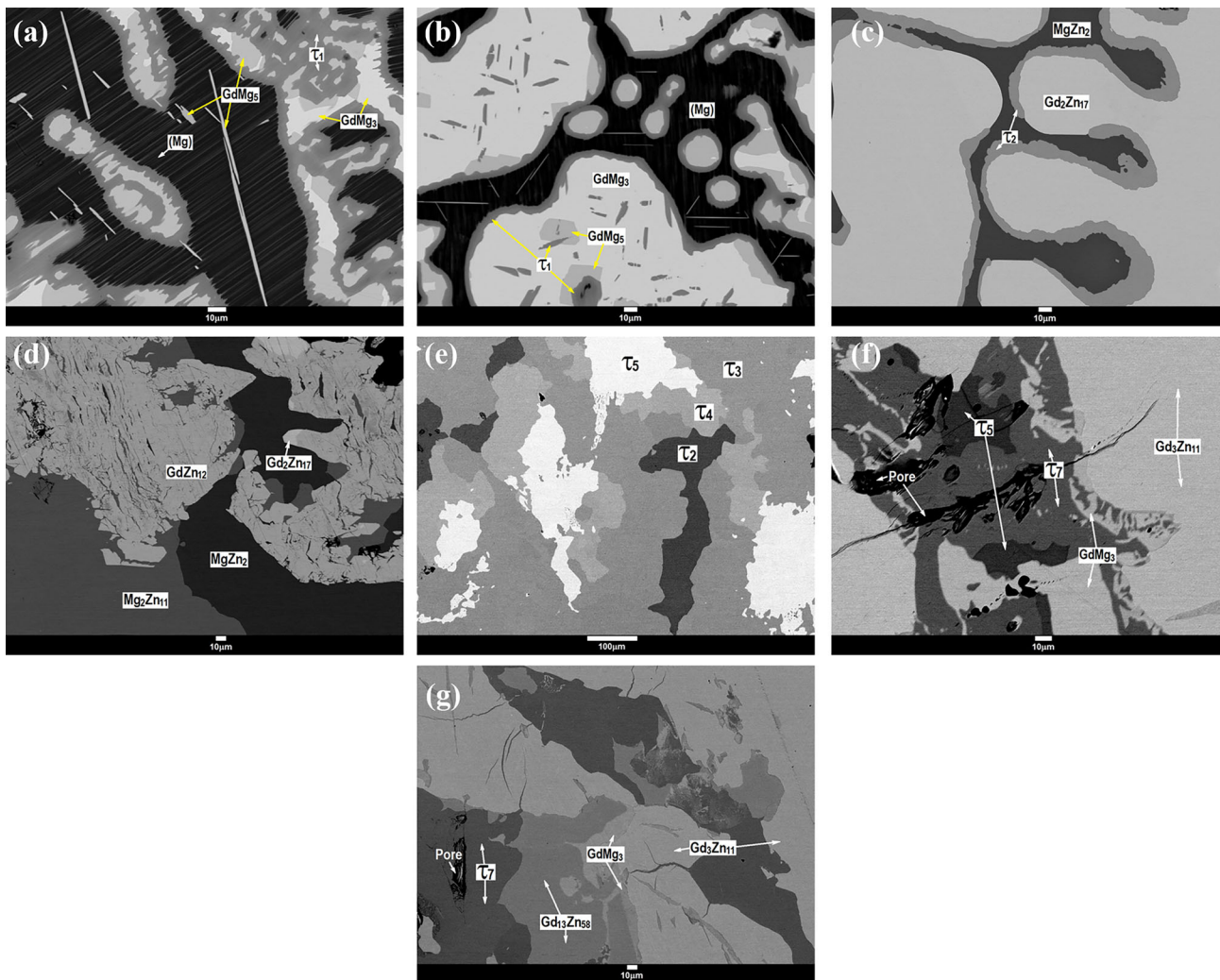


Fig. 3. BSE micrographs of the alloys annealed at 320°C. (a) Alloy #1 (300 days); (b) Alloy #3 (300 days); (c) Alloy #14 (100 days); (d) Alloy #15 (100 days); (e) Alloy #18 (100 days); (f) Alloy #29 (100 days) (g) Alloy #30 (100 days).

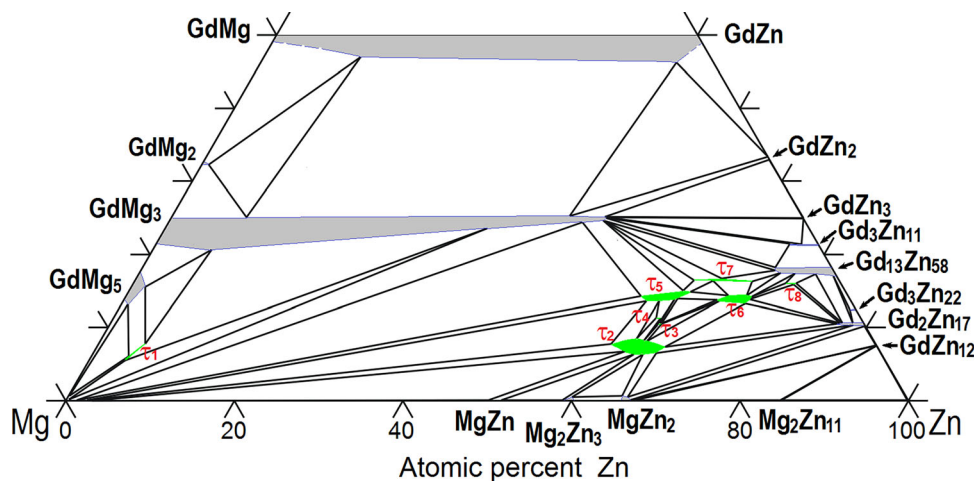


Fig. 4. The isothermal section at 320°C in the region below 50 at.% Gd.

**Table II. Summary of the ternary compounds in the Mg-Gd-Zn system**

Phase name/ composition range	Pearson symbol, space group	Lattice parameters (nm) / comments / references or alternative notation / references
$\tau_1$ (14H) Gd <sub>5.5-7.8</sub> Mg <sub>86.7-90.2</sub> Zn <sub>4.3-5.5</sub>	Hexagonal LPSO structure	$a = 0.325, c = 3.722$ at Gd <sub>11.0</sub> Mg <sub>80.9±1.0</sub> Zn <sub>8.1±1.0</sub> <sup>5</sup> X-phase (LPSO-14H) <sup>12-14</sup>
$\tau_2$ (Z-phase) Gd <sub>6.4-8.5</sub> Mg <sub>25.2-31.4</sub> Zn <sub>60.8-67.4</sub>	hP92 P6 <sub>3</sub> /mmc <sup>20</sup>	$A = 1.459, c = 0.884$ at Gd <sub>7.4</sub> Mg <sub>28.4</sub> Zn <sub>64.2</sub> <sup>16</sup> $A = 1.462, c = 0.871$ at Gd <sub>7.8</sub> Mg <sub>25.7</sub> Zn <sub>66.5</sub> <sup>17</sup> $A = 1.4633(2), c = 0.8761(2)$ at Gd <sub>7.7</sub> Mg <sub>28.6</sub> Zn <sub>63.8</sub> <sup>20</sup> Z-phase: (Gd <sub>7.4</sub> Mg <sub>28.4</sub> Zn <sub>64.2</sub> ) <sup>16</sup> ; $\mu$ -MgZnRE phases <sup>20</sup>
$\tau_3$ Gd <sub>10.5-10.6</sub> Mg <sub>24.0-24.6</sub> Zn <sub>65.0-65.5</sub>	P6 <sub>3</sub> /mmc <sup>21</sup>	Unknown, this work M-phase <sup>21</sup>
$\tau_4$ Gd <sub>11.3-11.5</sub> Mg <sub>23.5-24.2</sub> Zn <sub>64.4-65.1</sub>	P6 <sub>3</sub> /mmc <sup>21</sup>	Unknown, this work L-phase <sup>21</sup>
$\tau_5$ (F-phase) Gd <sub>13.6-15.1</sub> Mg <sub>18.4-24.6</sub> Zn <sub>61.1-66.7</sub>	cF480 F $\bar{4}3$ m <sup>14</sup>	$A = 1.966$ at Gd <sub>14.4</sub> Mg <sub>22.2</sub> Zn <sub>63.4</sub> <sup>16</sup> $A = 2.0415$ at Gd <sub>14.1</sub> Mg <sub>21.3</sub> Zn <sub>64.6</sub> <sup>17</sup> F-phase <sup>16</sup>
$\tau_6$ Gd <sub>13.3-14.4</sub> Mg <sub>11.5-15.8</sub> Zn <sub>70.4-74.2</sub>	— <sup>a</sup>	Unknown, this work
$\tau_7$ Gd <sub>16.4-16.7</sub> Mg <sub>10.4-17.2</sub> Zn <sub>66.3-73.3</sub>	— <sup>a</sup>	$A = 0.937, c = 0.977$ at Gd <sub>16</sub> Mg <sub>14</sub> Zn <sub>70</sub> <sup>15</sup> $A = 0.90962, c = 0.94, 112$ at Gd <sub>16.6</sub> Mg <sub>17.8</sub> Zn <sub>65.6</sub> <sup>22</sup> H <sub>2</sub> (Gd <sub>16</sub> Mg <sub>14</sub> Zn <sub>70</sub> ) <sup>15</sup>
$\tau_8$ Gd <sub>15.9-16.1</sub> Mg <sub>5.3-6.5</sub> Zn <sub>77.4-78.6</sub>	— <sup>a</sup>	Unknown, this work

<sup>a</sup>Indicates no data available in the literature.

been determined to be Gd<sub>5.5-7.8</sub>Mg<sub>86.7-90.2</sub>Zn<sub>4.3-5.5</sub> at 320°C according to the present results.

Three hexagonal phases were found and named  $\tau_2$ ,  $\tau_3$ , and  $\tau_4$ . The  $\tau_2$  phase has been named as the Z-phase<sup>16,17</sup> or the  $\mu$ -phase<sup>20</sup> in previous studies. Abe et al.<sup>21</sup> named  $\tau_2$ ,  $\tau_3$  and  $\tau_4$  as the S-phase, M-phase, and L-phase, respectively. The homogeneity ranges of  $\tau_2$ ,  $\tau_3$ , and  $\tau_4$  were determined to be Gd<sub>6.4-8.5</sub>Mg<sub>25.2-31.4</sub>Zn<sub>60.8-67.4</sub>, Gd<sub>10.5-10.6</sub>Mg<sub>24.0-24.6</sub>Zn<sub>65.0-65.5</sub>, and Gd<sub>11.3-11.5</sub>Mg<sub>23.5-24.2</sub>Zn<sub>64.4-65.1</sub>, respectively.

The  $\tau_5$  phase, labeled the F-phase,<sup>16,17</sup> has a composition range of Gd<sub>13.6-15.1</sub>Mg<sub>18.4-24.6</sub>Zn<sub>61.1-66.7</sub>. The composition range of  $\tau_7$  was determined to be Gd<sub>16.4-16.7</sub>Mg<sub>10.4-17.2</sub>Zn<sub>66.3-73.3</sub>. This phase is identical to the Gd<sub>16.6</sub>Mg<sub>17.8</sub>Zn<sub>65.6</sub> phase reported by Li et al.<sup>22</sup>

The phases  $\tau_6$  and  $\tau_8$  were measured to have the composition ranges of Gd<sub>13.3-14.4</sub>Mg<sub>11.5-15.8</sub>Zn<sub>70.4-74.2</sub> and Gd<sub>15.9-16.1</sub>Mg<sub>5.3-6.5</sub>Zn<sub>77.4-78.6</sub>, respectively. Their crystal structures have yet to be determined.

The icosahedral quasicrystalline phase (I-phase) was observed in the as-cast alloys,<sup>6,8,9,15</sup> especially under rapid solidification conditions such as melt-quenching.<sup>9</sup> Fisher et al.<sup>8</sup> and Gröbner et al.<sup>15</sup> considered the I-phase as a metastable phase, whereas Liu et al.<sup>7</sup> concluded that it is a stable phase, as they observed it in their as-cast and annealed alloys (at 440°C for 8 h). The composition of the I-phase was measured to be Gd<sub>11</sub>Mg<sub>29</sub>Zn<sub>60</sub> by Gröbner et al.,<sup>15</sup> Gd<sub>8.58</sub>Mg<sub>41.81</sub>Zn<sub>49.61</sub> by Liu et al.,<sup>7</sup> and Gd<sub>7.10</sub>Mg<sub>30</sub>Zn<sub>60-63</sub> by Saito et al.<sup>9</sup> In the present work,

no stable icosahedral quasicrystalline phase was found. In fact, the ternary compound  $\tau_2$  (Gd<sub>6.4-8.5</sub>Mg<sub>25.2-31.4</sub>Zn<sub>60.8-67.4</sub>) partially covers the compositions (Gd<sub>7</sub>Mg<sub>30</sub>Zn<sub>63</sub> and Gd<sub>8</sub>Mg<sub>30</sub>Zn<sub>62</sub>) of Saito et al.<sup>9</sup> Thus, the I-phases reported by Saito et al.<sup>9</sup> are metastable. In addition, the relatively short annealing time (8 h) by Liu et al.<sup>7</sup> is not sufficient to confirm that the I-phase is stable. Thus, it is concluded that the I phase in the Mg-Gd-Zn system is not stable.

### Phase Equilibria

Figure 3a and b show the BSE images of alloys #1 and #3, respectively. As labeled in Table I, the two alloys were taken from our previous work and were annealed at 500°C for 80 days,<sup>17</sup> and were re-annealed at 320°C for 300 days. According to our previous work,<sup>17</sup> alloys #1 and #3 are located in the two-phase fields of (Mg) + GdMg<sub>3</sub> at 500°C. At 320°C, these two alloys are in the three-phase equilibrium fields of (Mg) + GdMg<sub>5</sub> +  $\tau_1$  and of GdMg<sub>5</sub> +  $\tau_1$  + GdMg<sub>3</sub>, respectively. Thus, there is an invariant reaction (Mg) + GdMg<sub>3</sub> →  $\tau_1$  + GdMg<sub>5</sub> between 500°C and 320°C. The invariant transition (Mg) + GdMg<sub>3</sub> →  $\tau_1$  + GdMg<sub>5</sub> in the Mg-rich corner demonstrates the reason for the age hardening of the Mg-Gd-based magnesium alloys. In addition, the homogeneity range of the ternary phase  $\tau_1$  (14H) at 320°C (Gd<sub>5.5-7.8</sub>Mg<sub>86.7-90.2</sub>Zn<sub>4.3-5.5</sub>) becomes significantly larger than at 500°C (Gd<sub>5.5-6.2</sub>Mg<sub>89.2-90.0</sub>Zn<sub>4.3-4.7</sub>),<sup>17</sup> as shown in Fig. 4 and listed in Table II. It should be

noted that (Mg),  $\text{GdMg}_3$ ,  $\tau_1$ , and  $\text{GdMg}_5$  were found in alloys #1 and #3. One possibility is that the invariant reaction is at this temperature. However, it is more likely that these two alloys did not reach the equilibrium state. Increasing the annealing time of these alloys can certainly bring them to the full equilibrium state. However, in the present work, when the annealing time has reached 300 days, significant amounts of the metastable  $\text{GdMg}_3$  phase (in alloy #1) and (Mg) phase (in alloy #3) were found in the present work. Therefore, no attempt was made to further increase the annealing time.

It has been reported that a “ternary compound” W phase with the same crystal structure as  $\text{GdMg}_3$  forms at 500°C.<sup>12–14</sup> Thus, a two-phase equilibrium of the W and  $\text{GdMg}_3$  phases were observed, which was termed “phase separation”. In the present work, alloys #4–7 and #34–37 were designed to investigate the phase relationships between the W and  $\text{GdMg}_3$  phases at 320°C. However, the so-called phase separation was not found at 320°C. The maximum solubility of Zn in  $\text{GdMg}_3$  was measured to be 51.7%. Thus, whether the W phase is stable is questionable.

Figure 3c and d exhibit the BSE images of alloys #14 and #15, respectively. A typical peritectic microstructure formed during solidification was observed, as shown in Fig. 3c and d. Although the samples have been annealed at 500°C for 120 days and then at 320°C for up to 300 days, the peritectic microstructure remained clear due to the slow kinetics in alloy #14. Nevertheless, the three-phase conjunctions of  $\text{MgZn}_2 + \tau_2$  (Z-phase) +  $\text{Gd}_2\text{Zn}_{17}$  were detected in alloy #14. Four phases ( $\text{MgZn}_2$ ,  $\text{GdZn}_{12}$ ,  $\text{Mg}_2\text{Zn}_{11}$ , and  $\text{Gd}_2\text{Zn}_{17}$ ) were observed in alloy #15. According to the microstructure, the  $\text{Gd}_2\text{Zn}_{17}$  phase was the primary phase of a peritectic reaction and almost disappeared. Therefore, it is considered that  $\text{Gd}_2\text{Zn}_{17}$  is not a stable phase. A three-phase equilibrium of  $\text{MgZn}_2 + \text{GdZn}_{12} + \text{Mg}_2\text{Zn}_{11}$  was determined in alloy #15, as shown in Fig. 3d.

Alloy #18 was taken from the work at 500°C<sup>17</sup> and re-annealed at 320°C. This alloy was still composed of the four phases  $\tau_2$  to  $\tau_5$ , as shown in Fig. 3e. However, the equilibrium compositions of the specific phases changed slightly when the temperature was lowered from 500 to 320°C, indicating sluggish reaction kinetics. As shown in Fig. 4, it is hard to see the tie-triangles corresponding to the two three-phase equilibria of  $\tau_2 + \tau_3 + \tau_4$  and of  $\tau_3 + \tau_4 + \tau_5$ , as the two three-phase fields are very narrow. Since the alloy is far from the full equilibrium state, the present results for alloy #18 are tentative.

Figure 3f and g presents the BSE images of alloys #29 and #30, respectively. Alloy #29 was composed of four phases ( $\tau_5$ ,  $\tau_7$ ,  $\text{GdMg}_3$ , and  $\text{Gd}_3\text{Zn}_{11}$ ). From the microstructure, the  $\text{Gd}_3\text{Zn}_{11}$  is the primary precipitated phase and is transforming to other phases. In addition, the volume fraction of the

$\text{Gd}_3\text{Zn}_{11}$  is unusually small. Thus, it is concluded that the  $\text{Gd}_3\text{Zn}_{11}$  is not a stable phase. The three-phase equilibrium of  $\tau_5 + \tau_7 + \text{GdMg}_3$  was measured in alloy #29. The former was also detected in the above alloy #24 and is accepted in Fig. 4. Similarly, the three-phase equilibrium of  $\text{GdMg}_3 + \text{Gd}_{13}\text{Zn}_{58} + \text{Gd}_3\text{Zn}_{11}$  determined in alloy #30 is accepted in Fig. 4.

Compared with the isothermal section at 500°C of the Mg-Gd-Zn by Xu et al., the major difference is that the W phase was not stable at 320°C.

Discussions on the rest alloys can be found in the Supplementary Material (see supplementary Figure S1).

Based on the experimental data obtained in the present work, the partial isothermal section ( $x(\text{Gd}) < 50$  at.%) at 320°C is constructed in Fig. 4.

## CONCLUSION

The solid-state phase equilibria below 400°C of the Mg-Gd-Zn system is essential information for the understanding of the aging treatment of Mg-RE alloys. The phase equilibria at 320°C of the Mg-Gd-Zn system were studied, and the isothermal section at 320°C was constructed. Eight stable ternary phases ( $\tau_1$  to  $\tau_8$ ) formed at 320°C. The stabilities of the ternary compounds W and I were studied. The W phase ( $\text{Gd}_2\text{Mg}_3\text{Zn}_3$ ) phase was not found at 320°C according to the present results. The I phase was not found in the present work which indicates that the I phase is not stable in the Mg-Gd-Zn system.

Although the samples were annealed at 320°C for 310 days, some alloys (1, 3, 15, 18) have still not reached equilibrium, since more than three phases have been observed. Further studies are necessary.

The homogeneity ranges of the eight ternary compounds ( $\tau_1$  to  $\tau_8$ ) were determined:  $\text{Gd}_{5.5}7.8\text{Mg}_{86.7-90.2}\text{Zn}_{4.3-5.5}$  ( $\tau_1$ ),  $\text{Gd}_{6.4-8.5}\text{Mg}_{25.2-31.4}\text{Zn}_{60.8-67.4}$  ( $\tau_2$ ),  $\text{Gd}_{10.5-10.6}\text{Mg}_{24.0-24.6}\text{Zn}_{65.0-65.5}$  ( $\tau_3$ ),  $\text{Gd}_{11.3-11.5}\text{Mg}_{23.5-24.2}\text{Zn}_{64.4-65.1}$  ( $\tau_4$ ),  $\text{Gd}_{13.6-15.1}\text{Mg}_{18.4-24.6}\text{Zn}_{61.1-66.7}$  ( $\tau_5$ ),  $\text{Gd}_{13.3-14.4}\text{Mg}_{11.5-15.8}\text{Zn}_{70.4-74.2}$  ( $\tau_6$ ),  $\text{Gd}_{16.4-16.7}\text{Mg}_{10.4-17.2}\text{Zn}_{66.3-73.3}$  ( $\tau_7$ ), and  $\text{Gd}_{15.9-16.1}\text{Mg}_{5.3-6.5}\text{Zn}_{77.4-78.6}$  ( $\tau_8$ ), respectively.

The solubilities of Zn in  $\text{GdMg}_2$ ,  $\text{GdMg}_3$ , and  $\text{GdMg}_5$  were measured to be 0.8, 51.7, and 1.6 at.% Zn, respectively. The solubilities of Mg in  $\text{Gd}_3\text{Zn}_{11}$ ,  $\text{Gd}_{13}\text{Zn}_{58}$ ,  $\text{Gd}_3\text{Zn}_{22}$ ,  $\text{Gd}_2\text{Zn}_{17}$ , and  $\text{GdZn}_{12}$  were determined to be up to 3.3, 6.9, 0.7, 3.1, and 0.1 at.% Mg, respectively. The solubilities of Gd in  $\text{MgZn}$ ,  $\text{Mg}_2\text{Zn}_3$ ,  $\text{MgZn}_2$ , and  $\text{Mg}_2\text{Zn}_{11}$  are about 0.1, 0.5, 0.7, and 0.1 at.% Gd, respectively. The solubilities of Mg in the  $\text{GdZn}_2$  and  $\text{GdZn}_3$  phases are negligible.

The two previously reported equilibria (Mg) +  $\text{GdMg}_3 + \text{GdMg}_5$  and (Mg) +  $\text{GdMg}_3 + \tau_1$  in the Mg-rich corner at 500°C transform to (Mg) +  $\text{GdMg}_5 + \tau_1$  and  $\text{GdMg}_5 + \tau_1 + \text{GdMg}_3$  at 320°C, due to the invariant reaction of (Mg) +  $\text{GdMg}_3 \rightarrow$

$\text{GdMg}_5 + \tau_1$ . This phase transition is expected to favor the age hardening of the Mg-Gd-based

magnesium alloys, as more volume fraction of the strengthening phase  $\tau_1$  (14H) emerges during the aging treatment.

### SUPPLEMENTARY INFORMATION

The online version contains supplementary material available at <https://doi.org/10.1007/s11837-023-05737-2>.

### ACKNOWLEDGEMENTS

The financial supports from the China Hunan Provincial Science & Technology Department (Grant No 2020GK2051), Major Special Projects in Changsha Science and Technology Bureau (Grant No kh2103011), National key research and development program of China (2021YFB3502600) are greatly acknowledged.

### CONFLICT OF INTEREST

On behalf of all authors, the corresponding author states that there is no conflict of interest.

### REFERENCES

- W. Rong, Y. Zhang, Y. Wu, Y. Chen, T. Tang, L. Peng, and D. Li, *Mater. Charact.* 131, 380 (2017).
- D. Wu, R. Chen, and E. Han, *J. Alloy. Compd.* 509, 2856 (2011).
- J. Liu, L. Yang, C. Zhang, B. Zhang, T. Zhang, Y. Li, K. Wu, and F. Wang, *J. Alloy. Compd.* 782, 648 (2019).
- J. Wang, W. Jiang, Y. Ma, Y. Li, and S. Huang, *Mater. Chem. Phys.* 203, 352 (2018).
- Y. Wu, D. Lin, X. Zeng, L. Peng, and W. Ding, *J. Mater. Sci.* 44, 1607 (2009).
- Y. Tian, H. Huang, G. Yuan, and W. Ding, *J. Alloy. Compd.* 626, 42 (2015).
- Y. Liu, G. Yuan, C. Lu, and W. Ding, *Scripta Mater.* 55, 919 (2006).
- I. Fisher, Z. Islam, A. Panchula, K. Cheon, M. Kramer, P. Canfield, and A. Goldman, *Philos. Magaz. B* 77, 1601 (1998).
- H. Saito, K. Fukamichi, T. Goto, A. Tsai, A. Inoue, and T. Masumoto, *J. Alloy. Compd.* 252, 6 (1997).
- D. Wang, P. Fu, L. Peng, Y. Wang, and W. Ding, *Mater. Charact.* 153, 157 (2019).
- J.F. Nie, K. Oh-Ishi, X. Gao, and K. Hono, *Acta Mater.* 56, 6061 (2008).
- H. Qi, G. Huang, H. Bo, G. Xu, L. Liu, and Z. Jin, *J. Mater. Sci.* 47, 1319 (2012).
- Z. Zhu, and A.D. Pelton, *J. Alloy. Compd.* 652, 426 (2015).
- J. Gröbner, A. Kozlov, X.-Y. Fang, S. Zhu, J.-F. Nie, M.A. Gibson, and R. Schmid-Fetzer, *Acta Mater.* 90, 400 (2015).
- J. Gröbner, S. Zhu, J.-F. Nie, M.A. Gibson, and R. Schmid-Fetzer, *J. Alloy. Compd.* 675, 149 (2016).
- B. Liu, H. Li, Y. Ren, H. Xie, H. Pan, M. Jiang, and G. Qin, *J. Alloy. Compd.* 870, 159502 (2021).
- H. Xu, H.-L. Chen, P. Wang, and T. Zhou, *J. Alloy. Compd.* 884, 161048 (2021).
- H. Xu, J. Fan, H.-L. Chen, R. Schmid-Fetzer, F. Zhang, Y. Wang, Q. Gao, and T. Zhou, *J. Alloy. Compd.* 603, 100 (2014).
- H. Xu, Y. Du, Y. Tan, Y. He, S. Li, and Z. Xiang, *J. Alloy. Compd.* 425, 153 (2006).
- K. Sugiyama, K. Yasuda, T. Ohsuna, and K. Hiraga, *Zeit. für Kristallogr. Cryst. Mater.* 213, 537 (1998).
- E. Abe, H. Takakura, A. Singh, and A. Tsai, *J. Alloy. Compd.* 283, 169 (1999).
- M. Li, D. Deng, and K. Kuo, *J. Alloy. Compd.* 414, 66 (2006).

**Publisher's Note** Springer Nature remains neutral with regard to jurisdictional claims in published maps and institutional affiliations.

Springer Nature or its licensor (e.g. a society or other partner) holds exclusive rights to this article under a publishing agreement with the author(s) or other rightsholder(s); author self-archiving of the accepted manuscript version of this article is solely governed by the terms of such publishing agreement and applicable law.